Solid solutions with AlB_2-type structure in *R*–Ag–Al–Ge systems (*R* = Ce, Pr, Nd, Sm)

Roksolana KOZAK[1]*, Yaroslav TOKAYCHUK[1], Mykola MANYAKO[1], Roman GLADYSHEVSKII[1]

[1] *Department of Inorganic Chemistry, Ivan Franko National University of Lviv,*
   Kyryla i Mefodiya St. 6, 79005 Lviv, Ukraine
* *Corresponding author. E-mail: r-kozak@ukr.net*

An investigation of the quaternary systems *R*–Ag–Al–Ge (*R* = Ce, Pr, Nd, Sm) at 873 K led to the discovery of three complete solid solutions based on ternary germanides, $CeAg_{0.8}Ge_{1.2}$-$CeAl_{1.6-1.5}Ge_{0.4-0.5}$, $PrAg_{0.8}Ge_{1.2}$-$PrAl_{1.55-1.48}Ge_{0.45-0.52}$, and $NdAg_{0.7}Ge_{1.3}$-$NdAl_{1.63-1.50}Ge_{0.37-0.50}$, and a quaternary compound, $SmAg_{0.55-0.36}Al_{0.43-0.80}Ge_{1.02-0.84}$, with AlB_2-type structure (Pearson symbol *hP*3, space group *P*6/*mmm*). The crystal structure of the solid solution in the system Pr-Ag-Al-Ge was refined for the composition $PrAg_{0.38}Al_{0.80}Ge_{0.82}$ from X-ray powder (*a* = 0.43368(5), *c* = 0.41929(7) nm) and single-crystal (*a* = 0.4318(1), *c* = 0.4191(1) nm) diffraction data. Within the homogeneity range the contact distances between small-size atoms decrease with increasing Al and decreasing Ag and Ge content. The valence electron concentration per atom of the statistical mixture Ag+Al+Ge increases from 4.30 to 4.76 within the same range.

Rare-earth / Silver / Aluminum / Germanium / Solid solution / X-ray diffraction / Crystal structure

Introduction

The formation of ternary compounds with hexagonal AlB_2-type structure (*hP*3, *P*6/*mmm*) has been reported for the RAg_2–RGe_2 and RAl_2–RGe_2 cross-sections of the *R*–Ag–Ge and *R*–Al–Ge systems (where *R* is a light rare-earth metal) [1-7]. The compounds in the systems *R*–Ag–Ge, except for *R* = Sm, are characterized by point compositions: $LaAg_{0.8}Ge_{1.2}$ (773 K), $CeAg_{0.8}Ge_{1.2}$ (773 K), $PrAg_{0.8}Ge_{1.2}$ (873 K), $NdAg_{0.7}Ge_{1.3}$ (1073 K), EuAgGe (673 K), $EuAg_{0.8}Ge_{1.2}$ (973 K), and $GdAg_{0.6}Ge_{1.4}$ (873 K) [1-3]. On the contrary, the alumogermanides of La, Ce, Pr, Nd, and Eu have significant homogeneity ranges: $LaAl_{1.8-1.5}Ge_{0.2-0.5}$ (773 K), $CeAl_{1.6-1.5}Ge_{0.4-0.5}$ (773 K), $PrAl_{1.55-1.48}Ge_{0.45-0.52}$ (673 and 873 K), $NdAl_{1.63-1.50}Ge_{0.37-0.50}$ (1273 K), and $EuAl_{1.08-1.00}Ge_{0.92-1.00}$ (873 K) [4-7]. The isotypic compound in the Sm–Al–Ge system has the point composition $SmAl_{1.5}Ge_{0.5}$ (1273 K) [4]. Literature data show the existence of numerous AlB_2-type compounds in related ternary systems. For instance, in the *R*–{Fe,Co,Zn}–Ge systems the following compounds have been reported: $RFe_{0.67}Ge_{1.33}$ for *R* = La, Nd, Sm (1873 K), $RCo_{0.5}Ge_{1.5}$ for *R* = Ce, Pr, Nd (873 K), $RZn_{1.5}Ge_{0.5}$ for *R* = La, Ce, Pr, Nd, Sm (1073 K) [1]. A modulated structure derived from the AlB_2 type was described in [8] for the quaternary compound $Pr(Ni_{0.20}Al_{0.30}Ge_{0.50})_{1.8}$. The existence of the complete solid solution $PrAg_{0.8}Ge_{1.2}$–

$PrAl_{1.55-1.48}Ge_{0.45-0.52}$ (873 K) and the quaternary compound $SmAg_{0.55-0.36}Al_{0.43-0.80}Ge_{1.02-0.84}$ (873 K) with AlB_2-type structure was briefly reported in [9-11]. The aim of the present work was in addition to look for regularities in the formation of the AlB_2-type compounds in the quaternary systems {Ce,Pr,Nd,Sm}–Ag–Al–Ge.

Experimental

Two three-component and 23 four-component alloys containing 33.3 at.% rare-earth element were synthesized by arc-melting the elements (Ce, Pr, Nd, Sm ≥ 99.83 wt.%, Al ≥ 99.985 wt.%, Ag and Ge ≥ 99.999 wt.%) under argon atmosphere. The samples were annealed at 873 K in evacuated quartz ampoules for 1 month and subsequently quenched in cold water. The weight losses during the preparation of the samples were less than 1 % of the total mass, which was 1 g for each alloy.

Phase analysis was carried out using X-ray powder diffraction data collected on a diffractometer DRON-2.0M (Fe *K*α radiation) in the angular range $20 \leq 2\theta \leq 100°$ with the step 0.05°. The profile and structural parameters were refined by the Rietveld method using the program DBWS-9807 [12]. X-ray single-crystal diffraction data were collected in the *ω*-2*θ* scan mode on a four-circle CAD-4T diffractometer (graphite

Table 1 Phases detected in alloys of the Ce–Ag–Al–Ge system at 873 K, 33.3 at.% Ce.

No.	Sample composition, at.%	Phase	Structure type	Unit-cell parameters		
				a, nm	c, nm	V, nm^3
1	$Ce_{33.3}Ag_{26.7}Ge_{40.0}$	**CeAg$_{0.8}$Ge$_{1.2}$**	AlB₂	0.43900(5)	0.41305(6)	0.06894(2)
		CeAgGe	LiGaGe	0.45350(9)	0.7725(3)	0.13759(6)
2	$Ce_{33.3}Ag_{23.3}Al_{6.7}Ge_{36.7}$	**CeAg$_{0.70}$Al$_{0.20}$Ge$_{1.10}$**	AlB₂	0.43901(6)	0.41407(8)	0.06911(2)
		CeAgGe	LiGaGe	0.4506(1)	0.7834(8)	0.1377(2)
3	$Ce_{33.3}Ag_{20.0}Al_{13.3}Ge_{33.4}$	**CeAg$_{0.60}$Al$_{0.40}$Ge$_{1.00}$**	AlB₂	0.43832(7)	0.41603(9)	0.06922(2)
4	$Ce_{33.3}Ag_{16.7}Al_{20.0}Ge_{30.0}$	**CeAg$_{0.50}$Al$_{0.60}$Ge$_{0.90}$**	AlB₂	0.43619(6)	0.42133(8)	0.06942(2)
5	$Ce_{33.3}Ag_{13.3}Al_{26.7}Ge_{26.7}$	**CeAg$_{0.40}$Al$_{0.80}$Ge$_{0.80}$**	AlB₂	0.43487(6)	0.42474(7)	0.06956(2)
6	$Ce_{33.3}Ag_{8.0}Al_{36.7}Ge_{22.0}$	**CeAg$_{0.24}$Al$_{1.10}$Ge$_{0.66}$**	AlB₂	0.43543(7)	0.42603(9)	0.06995(2)
7	$Ce_{33.3}Ag_{2.7}Al_{46.7}Ge_{17.3}$	**CeAg$_{0.08}$Al$_{1.40}$Ge$_{0.52}$**	AlB₂	0.43480(5)	0.42953(7)	0.07032(2)

Table 2 Phases detected in alloys of the Pr–Ag–Al–Ge system at 873 K, 33.3 at.% Pr.

No.	Sample composition, at.%	Phase	Structure type	Unit-cell parameters		
				a, nm	c, nm	V, nm^3
1	$Pr_{33.3}Ag_{23.3}Al_{6.7}Ge_{36.7}$	**PrAg$_{0.70}$Al$_{0.20}$Ge$_{1.10}$**	AlB₂	0.43722(6)	0.40981(7)	0.06785(2)
2	$Pr_{33.3}Ag_{16.7}Al_{16.7}Ge_{33.3}$	**PrAg$_{0.50}$Al$_{0.50}$Ge$_{1.00}$**	AlB₂	0.43415(6)	0.41652(8)	0.06799(2)
3	$Pr_{33.3}Ag_{13.3}Al_{20.0}Ge_{33.4}$	**PrAg$_{0.40}$Al$_{0.60}$Ge$_{1.00}$**	AlB₂	0.43215(8)	0.41858(9)	0.06769(3)
4	$Pr_{33.3}Ag_{12.7}Al_{26.7}Ge_{27.3}$	**PrAg$_{0.38}$Al$_{0.80}$Ge$_{0.82}$**	AlB₂	0.43368(5)	0.41929(7)	0.06830(2)
5	$Pr_{33.3}Ag_{8.4}Al_{33.3}Ge_{25.0}$	**PrAg$_{0.25}$Al$_{1.00}$Ge$_{0.75}$**	AlB₂	0.43253(6)	0.42244(7)	0.06844(2)
6	$Pr_{33.3}Ag_{3.3}Al_{43.4}Ge_{20.0}$	**PrAg$_{0.10}$Al$_{1.30}$Ge$_{0.60}$**	AlB₂	0.43288(9)	0.42389(9)	0.06880(2)

monochromator, Mo *K*α radiation). An analytical absorption correction was applied. A full-matrix least-squares refinement of the structural parameters was performed on F^2 using the program SHELXL-97 [13]. An energy-dispersive X-ray analysis was performed on a REM-106I electron scanning microscope.

Results and discussion

The phases identified in the samples synthesized at 873 K in the *R*–Ag–Al–Ge systems (*R* = Ce, Pr, Nd, Sm) and their refined unit-cell parameters as obtained from X-ray powder diffraction data are listed in Tables 1-4. The existence of the ternary compounds CeAg$_{0.8}$Ge$_{1.2}$ (structure type AlB₂, *P6/mmm*), CeAgGe (LiGaGe, *P6₃mc*), Nd₃Ag₄Ge₄ (Gd₃Cu₄Ge₄, *Immm*), NdAg$_{0.7}$Ge$_{1.3}$ (AlB₂, *P6/mmm*), and NdAg$_{1.4}$Ge$_{0.6}$ (Fe₂P, *P-62m*) was confirmed based on the phase analysis of the ternary samples Ce$_{33.3}$Ag$_{26.7}$Ge$_{40.0}$ and Nd$_{33.3}$Ag$_{23.4}$Ge$_{43.3}$. Differently from [3], we observed the existence of the ternary compound NdAg$_{0.7}$Ge$_{1.3}$ at a lower temperature (873 K). The quaternary alloys were single-phase samples containing phases with AlB₂-type structure, except Ce$_{33.3}$Ag$_{23.3}$Al$_{6.7}$Ge$_{36.7}$ and some alloys from the Sm‑Ag‑Al‑Ge system, which contained as additional phases CeAgGe or Sm₃Ag₄Ge₄ (Gd₃Cu₄Ge₄, *Immm*) and SmAg$_{1.4}$Ge$_{0.6}$ (Fe₂P, *P-62m*). Consequently, the following solid solutions with AlB₂-type structure were found at 33.3 at.% *R* and 873 K in the systems {Ce,Pr,Nd,Sm}–Ag–Al–Ge: CeAg$_{0.8}$Ge$_{1.2}$–CeAl$_{1.6-1.5}$Ge$_{0.4-0.5}$, PrAg$_{0.8}$Ge$_{1.2}$–PrAl$_{1.55-1.48}$Ge$_{0.45-0.52}$, NdAg$_{0.7}$Ge$_{1.3}$–NdAl$_{1.63-1.50}$Ge$_{0.37-0.50}$ and SmAg$_{0.55-0.36}$Al$_{0.43-0.80}$Ge$_{1.02-0.84}$.

The variation of the unit-cell parameters within the homogeneity ranges of the AlB₂-type compounds in the quaternary systems {Ce,Pr,Nd,Sm}–Ag–Al–Ge is shown in Fig. 1. The *a*-parameter decreases with increasing Al content (0-54.3 at.%) and decreasing Ag and Ge content (26.7-0 and 43.3-12.3 at.%, respectively), whereas the *c*-parameter increases. In the AlB₂-type structure each small-size atom (in our case a statistical mixture of Ag, Al, and Ge atoms) has three "homoatomic" bonds, so that infinite graphite-like planar nets perpendicular to the 6-fold axes are formed. The large-size atoms (rare-earth metal atoms here) are situated between the nets and form trigonal prisms. All the space in the structure is filled up by R_6 trigonal prisms, the centers of which are occupied by atoms of the statistical mixture *M* = Ag+Al+Ge. The replacement of Ag and Ge atoms (covalent radii r = 0.134 and 0.122 nm, respectively) by Al atoms (r = 0.118 nm) directly influences the *a*-parameter, which reflects the contact distances between small-size atoms in the structure ($\delta_{M-M} = a/\sqrt{3}$). The trigonal prisms are slightly compressed along the prism axis ($c/a < 1$), however, the c/a ratio increases with increasing Al content. An important criterion for the formation of solid solutions, in addition to the atom-size factor, is the number of valence electrons. For the AlB₂-type phases studied here the valence electron concentration per atom of the statistical mixture *M* = Ag+Al+Ge (VEC$_A$ [14]) is in the range 4.30-4.76. The replacement of Ag atoms with one valence electron and Ge atoms with four valence electrons in the ratio Ag:Ge = 1:1, by Al atoms with three valence electrons leads to an increase of VEC$_A$. It should be noticed that for other extended solid solutions in the systems

◑ CeAg$_{0.8}$Ge$_{1.2}$–CeAl$_{1.6-1.5}$Ge$_{0.4-0.5}$
○ PrAg$_{0.8}$Ge$_{1.2}$–PrAl$_{1.55-1.48}$Ge$_{0.45-0.52}$
● NdAg$_{0.7}$Ge$_{1.3}$–NdAl$_{1.63-1.50}$Ge$_{0.37-0.50}$
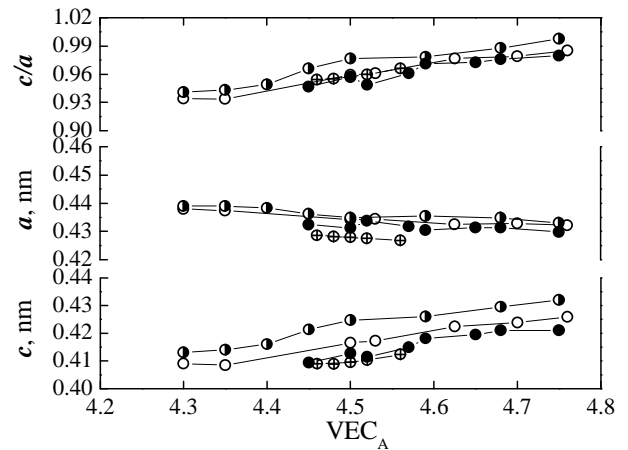⊕ SmAg$_{0.55-0.36}$Al$_{0.43-0.80}$Ge$_{1.02-0.84}$

Fig. 1 Unit-cell parameters within the homogeneity ranges of the AlB$_2$-type compounds in the quaternary systems {Ce,Pr,Nd,Sm}–Ag–Al–Ge as a function of the valence electron concentration VEC$_A$.

Table 3 Phases detected in alloys of the Nd–Ag–Al–Ge system at 873 K, 33.3 at.% Nd.

No.	Sample composition, at.%	Phase	Structure type	Unit-cell parameters			
				a, nm	*b*, nm	*c*, nm	*V*, nm^3
1	Nd$_{33.3}$Ag$_{23.4}$Ge$_{43.3}$	**Nd$_3$Ag$_4$Ge$_4$**	Gd$_3$Cu$_4$Ge$_4$	0.4413(1)	0.7111(2)	1.4667(4)	0.4603(2)
		NdAg$_{0.7}$Ge$_{1.3}$	AlB$_2$	0.4324(1)	–	0.4094(1)	0.06627(3)
		NdAg$_{1.4}$Ge$_{0.6}$	ZrNiAl	0.7268(2)	–	0.4305(2)	0.1969(1)
2	Nd$_{33.3}$Ag$_{20.0}$Al$_{6.7}$Ge$_{40.0}$	**NdAg$_{0.60}$Al$_{0.20}$Ge$_{1.20}$**	AlB$_2$	0.43121(7)	–	0.41274(9)	0.06646(2)
3	Nd$_{33.3}$Ag$_{17.3}$Al$_{13.3}$Ge$_{36.0}$	**NdAg$_{0.52}$Al$_{0.40}$Ge$_{1.08}$**	AlB$_2$	0.43379(6)	–	0.41144(8)	0.06705(2)
4	Nd$_{33.3}$Ag$_{14.0}$Al$_{20.0}$Ge$_{32.7}$	**NdAg$_{0.42}$Al$_{0.60}$Ge$_{0.98}$**	AlB$_2$	0.43177(5)	–	0.41493(6)	0.06700(1)
5	Nd$_{33.3}$Ag$_{11.3}$Al$_{26.7}$Ge$_{28.7}$	**NdAg$_{0.34}$Al$_{0.80}$Ge$_{0.86}$**	AlB$_2$	0.43048(5)	–	0.41811(6)	0.06710(1)
6	Nd$_{33.3}$Ag$_{6.7}$Al$_{36.7}$Ge$_{23.3}$	**NdAg$_{0.20}$Al$_{1.10}$Ge$_{0.70}$**	AlB$_2$	0.43138(4)	–	0.41951(5)	0.06761(1)
7	Nd$_{33.3}$Ag$_{2.7}$Al$_{46.7}$Ge$_{17.3}$	**NdAg$_{0.08}$Al$_{1.40}$Ge$_{0.52}$**	AlB$_2$	0.43138(5)	–	0.42100(6)	0.06785(1)

Table 4 Phases detected in alloys of the Sm–Ag–Al–Ge system at 873 K, 33.3 at.% Sm.

No.	Sample composition, at.%	Phase	Structure type	Unit-cell parameters			
				a, nm	*b*, nm	*c*, nm	*V*, nm^3
1	Sm$_{33.3}$Ag$_{20.0}$Al$_{12.0}$Ge$_{34.7}$	**SmAg$_{0.55}$Al$_{0.43}$Ge$_{1.02}$**	AlB$_2$	0.42860(6)	–	0.4090(7)	0.06507(2)
		Sm$_3$Ag$_4$Ge$_4$	Gd$_3$Cu$_4$Ge$_4$	0.4427(1)	0.6978(2)	1.4572(4)	0.4501(2)
		SmAg$_{1.4}$Ge$_{0.6}$	ZrNiAl	0.7145(2)	–	0.4322(1)	0.1911(1)
2	Sm$_{33.3}$Ag$_{16.7}$Al$_{16.7}$Ge$_{33.3}$	**SmAg$_{0.50}$Al$_{0.50}$Ge$_{1.00}$**	AlB$_2$	0.42793(4)	–	0.40949(6)	0.06494(1)
		Sm$_3$Ag$_4$Ge$_4$	Gd$_3$Cu$_4$Ge$_4$	0.4389(1)	0.7048(2)	1.4489(3)	0.4482(2)
		SmAg$_{1.4}$Ge$_{0.6}$	ZrNiAl	0.7185(1)	–	0.4274(1)	0.19111(7)
3	Sm$_{33.3}$Ag$_{16.0}$Al$_{20.0}$Ge$_{30.7}$	**SmAg$_{0.48}$Al$_{0.60}$Ge$_{0.92}$**	AlB$_2$	0.42812(6)	–	0.40893(9)	0.06491(2)
		SmAg$_{1.4}$Ge$_{0.6}$	ZrNiAl	0.7161(1)	–	0.4304(1)	0.19114(6)
		Sm$_3$Ag$_4$Ge$_4$	Gd$_3$Cu$_4$Ge$_4$	0.4394(1)	0.7042(2)	1.4493(4)	0.4484(2)
4	Sm$_{33.3}$Ag$_{14.0}$Al$_{23.3}$Ge$_{29.4}$	**SmAg$_{0.42}$Al$_{0.70}$Ge$_{0.88}$**	AlB$_2$	0.42756(3)	–	0.41030(4)	0.06496(1)
		SmAg$_{1.4}$Ge$_{0.6}$	ZrNiAl	0.71165(9)	–	0.43434(9)	0.19051(5)
		Sm$_3$Ag$_4$Ge$_4$	Gd$_3$Cu$_4$Ge$_4$	0.4442(1)	0.6954(2)	1.4599(6)	0.4510(3)
5	Sm$_{33.3}$Ag$_{12.0}$Al$_{26.7}$Ge$_{28.0}$	**SmAg$_{0.36}$Al$_{0.80}$Ge$_{0.84}$**	AlB$_2$	0.42676(5)	–	0.41233(6)	0.06503(1)
		Sm$_3$Ag$_4$Ge$_4$	Gd$_3$Cu$_4$Ge$_4$	0.4447(2)	0.6949(3)	1.4629(6)	0.4521(3)
		SmAg$_{1.4}$Ge$_{0.6}$	ZrNiAl	0.7115(1)	–	0.4351(1)	0.19074(8)

{Pr,Sm}–Ag–Al–Ge at 33.3 at.% *R* and 873 K, VEC$_A$ = 3.65-4.17 (Fe$_2$P-type structures) and 4.77-5.00 (α-ThSi$_2$-type structures).

The crystal structure of the PrAg$_{0.8}$Ge$_{1.2}$–PrAl$_{1.55-1.48}$Ge$_{0.45-0.52}$ solid solution was investigated by X-ray powder and single-crystal diffraction. The results of the structure refinement for the polycrystalline sample of composition Pr$_{33.3}$Ag$_{12.7}$Al$_{26.7}$Ge$_{27.3}$ are presented in Table 5. A pseudo-Voigt function with four parameters was used for the profile refinement. Atomic coordinates and isotropic displacement parameters are listed in Table 6

Table 5 Details of the structure refinement for the polycrystalline sample Pr$_{33.3}$Ag$_{12.7}$Al$_{26.7}$Ge$_{27.3}$ (diffractometer DRON-2.0M, Fe *K*α radiation).

Phase		PrAg$_{0.38}$Al$_{0.80}$Ge$_{0.82}$
Space group		*P6/mmm*
Unit-cell parameters	*a*, nm	0.43368(5)
	c, nm	0.41929(7)
	V, nm^3	0.06830(2)
Formula units per cell *Z*		1
Density *D*$_X$, g cm^{-3}		6.394
Texture parameter *G*		1.062(8) [001]
FWHM parameters *U, V, W*		0.23(2), 0, 0.029(4)
Mixing parameter *η*		0.63(4)
Asymmetry parameter *C*$_M$		-0.19(4)
Number of refined parameters		11
Reliability factors *R*$_B$, *R*$_p$, *R*$_{wp}$		0.0908, 0.0468, 0.0580
Goodness of fit *S*		0.61

Table 6 Atomic coordinates and isotropic displacement parameters for PrAg$_{0.38}$Al$_{0.80}$Ge$_{0.82}$ (powder data, structure type AlB$_2$, Pearson symbol *hP*3, space group *P6/mmm*, *a* = 0.43368(5), *c* = 0.41929(7) nm).

Site	Wyckoff position	*x*	*y*	*z*	*B*$_{iso}$, 10^{-2} nm^2
Pr	1*a*	0	0	0	0.5(2)
M	2*d*	1/3	2/3	1/2	1.3(2)

M = 0.19Ag + 0.40Al + 0.41Ge

Table 7 Interatomic distances for PrAg$_{0.38}$Al$_{0.80}$Ge$_{0.82}$ (powder data).

Atoms		*δ*, nm
Pr	-12 *M*	0.32657(3)
	-2 Pr	0.41932(6)
	-6 Pr	0.43367(5)
M	-3 *M*	0.25038(3)
	-6 Pr	0.32657(3)

M = 0.19Ag + 0.40Al + 0.41Ge

and selected interatomic distances are given in Table 7. In the AlB$_2$-type structure the small-size atoms occupy one Wyckoff position (2*d*) and in the refinement the Ag:Al:Ge ratio was fixed according to the nominal composition of the alloy (PrAg$_{0.38}$Al$_{0.80}$Ge$_{0.82}$). An energy-dispersive X-ray analysis showed good agreement between the nominal composition of the sample and the composition of the quaternary phase (Pr$_{33(2)}$Ag$_{14(2)}$Al$_{29(4)}$Ge$_{24(3)}$). A backscattered electron image of the sample Pr$_{33.3}$Ag$_{12.7}$Al$_{26.7}$Ge$_{27.3}$ is presented in Fig. 2 and the observed, calculated and difference X-ray powder diffraction patterns of the same alloy are shown in Fig. 3. Experimental details of a structure refinement based on diffraction data collected for a single crystal extracted from the same alloy are listed in Table 8. No superstructure or satellite reflections were observed. Atomic coordinates and equivalent isotropic displacement parameters assuming an AlB$_2$-type structure without vacancies are presented in Table 9,
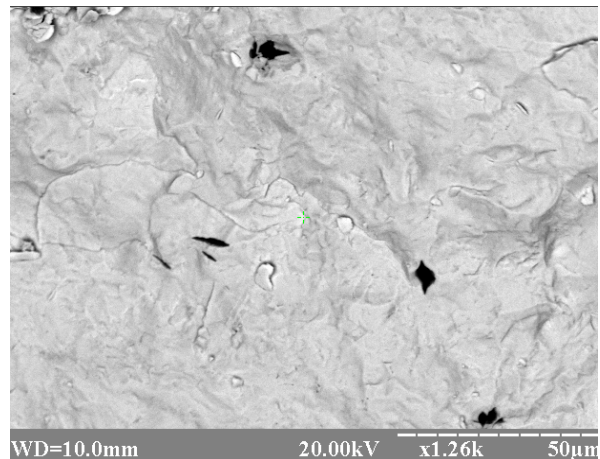

Fig. 2 Backscattered electron image of the sample Pr$_{33.3}$Ag$_{12.7}$Al$_{26.7}$Ge$_{27.3}$.

Table 8 Details of the data collection and structure refinement for PrAg$_{0.38}$Al$_{0.80}$Ge$_{0.82}$ (single-crystal data, diffractometer CAD-4T, Mo *K*α radiation).

Space group		*P*6/*mmm*
Unit-cell parameters	*a*, nm	0.4318(1)
	c, nm	0.4191(1)
	V, nm^3	0.06767(3)
Formula units per cell *Z*		1
Density *D*$_X$, g cm^{-3}		6.454
Absorption coefficient *μ*, mm^{-1}		24.96
Crystal size, mm		0.08 × 0.07 × 0.05
Data collection method		*ω*-2*θ* scan
Number of measured reflections		1241
Number of independent reflections		146
Number of reflections with *I* >2*σ*(*I*)		141
Factor *R*$_{int}$		0.0890
Range *h*, *k*, *l*		-8 ≤ *h* ≤ 7, -2 ≤ *k* ≤ 8, -8 ≤ *l* ≤ 8
Refinement on		*F*^{2}
Reliability factors	*R* (for *I* >2*σ*(*I*))	0.0346 (0.0337)
	wR	0.0641 (0.0639)
Goodness of fit *S*		1.176
Number of refined parameters		7
Weighting scheme		$w = 1/[(\sigma F_o)^2 + (0.0133P)^2]$
		$(P = (F_o^2 + 2F_c^2)/3)$
Extinction coefficient		0.08(2)
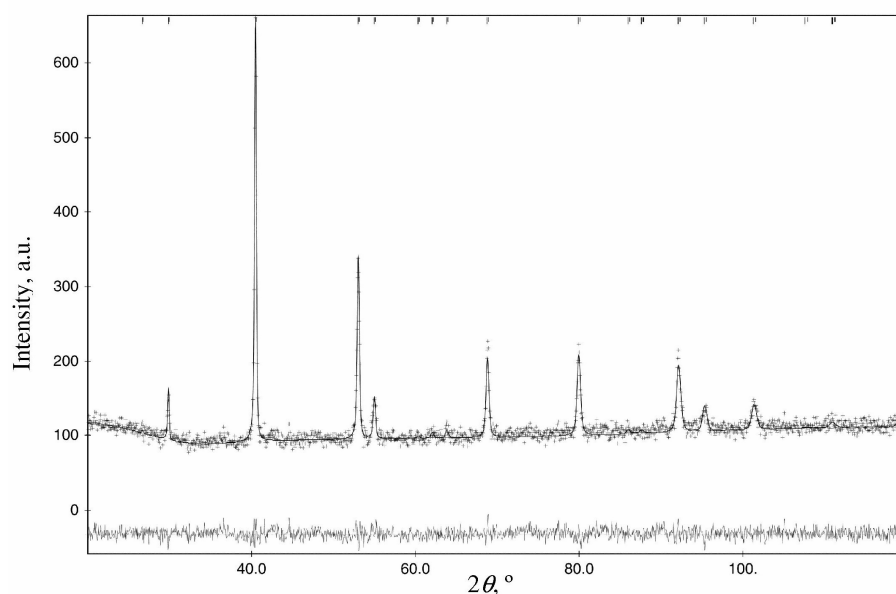
Fig. 3 Observed (dots), calculated (line) and difference (bottom) X-ray powder diffraction patterns for the Pr$_{33.3}$Ag$_{12.7}$Al$_{26.7}$Ge$_{27.3}$ sample (Fe *K*α radiation).

anisotropic displacement parameters and selected interatomic distances are listed in Tables 10 and 11, respectively. In this case the Ag:Al:Ge ratio was not fixed but the occupancy of the site was refined as a mixture between the heaviest (Ag) and the lightest (Al) elements. The refined composition 0.50(1)Ag + 0.50(1)Al corresponds to an average number of electrons of 30.0(3) for the atoms in the 2*d* site (to be compared with 27 electrons used for the refinement on

powder diffraction data).

As can be seen from Tables 11-15, the distances between *M* atoms correspond to the average covalent radius of the small-size atoms (r_{av} = (xr_{Ag}+yr_{Al}+zr_{Ge})/(x+y+z), where x, y and z are the relative quantities of Ag, Al and Ge in the statistical mixture). These distances are similar to those in the pure metals (δ_{Ag-Ag} = 0.289, δ_{Al-Al} = 0.286, δ_{Ge-Ge} = 0.245 nm).

Table 9 Atomic coordinates and equivalent displacement parameters for PrAg$_{0.38}$Al$_{0.80}$Ge$_{0.82}$ (single-crystal data, structure type AlB$_2$, Pearson symbol *hP*3, space group *P6/mmm*, *a* = 0.4318(1), *c* = 0.4191(1) nm).

Site	Wyckoff position	*x*	*y*	*z*	U_{eq}, 10^{-2} nm^2
Pr	1*a*	0	0	0	0.0072(2)
M	2*d*	1/3	2/3	1/2	0.0185(5)

M = 0.50(1)Ag + 0.50(1)Al used for the refinement

Table 10 Anisotropic displacement parameters (10^{-2} nm^2) for PrAg$_{0.38}$Al$_{0.80}$Ge$_{0.82}$ (single-crystal data).

Site	U_{11}	U_{22}	U_{33}	U_{12}	U_{13}	U_{23}
Pr	0.0065(2)	0.0065(2)	0.0101(3)	0.0032(1)	0	0
M	0.0091(5)	0.0091(5)	0.0374(8)	0.0045(2)	0	0

M = 0.50(1)Ag + 0.50(1)Al

Table 11 Interatomic distances for PrAg$_{0.38}$Al$_{0.80}$Ge$_{0.82}$ (single-crystal data).

Atoms		δ, nm
	-12 *M*	0.32566(6)
Pr	-2 Pr	0.4191(1)
	-6 Pr	0.4318(1)
M	-3 *M*	0.24930(7)
	-6 Pr	0.32566(6)

M = 0.50(1)Ag + 0.50(1)Al

Table 12 Interaxial ratio *c/a*, valence electron concentration VEC$_A$, contact distances between small atoms δ_{M-M}, and sum of the average covalent radii 2r_M for the solid solution CeAg$_{0.8}$Ge$_{1.2}$-CeAl$_{1.6-1.5}$Ge$_{0.4-0.5}$.

Composition	*c/a*	VEC$_A$	δ_{M-M}, nm	2r_M, nm
CeAg$_{0.80}$Ge$_{1.20}$	0.9409	4.30	0.2535	0.2536
CeAg$_{0.70}$Al$_{0.20}$Ge$_{1.10}$	0.9432	4.35	0.2535	0.2516
CeAg$_{0.60}$Al$_{0.40}$Ge$_{1.00}$	0.9492	4.40	0.2531	0.2496
CeAg$_{0.50}$Al$_{0.60}$Ge$_{0.90}$	0.9659	4.45	0.2518	0.2476
CeAg$_{0.40}$Al$_{0.80}$Ge$_{0.80}$	0.9767	4.50	0.2511	0.2456
CeAg$_{0.24}$Al$_{1.10}$Ge$_{0.66}$	0.9784	4.59	0.2514	0.2425
CeAg$_{0.08}$Al$_{1.40}$Ge$_{0.52}$	0.9879	4.68	0.2510	0.2394
CeAl$_{1.50}$Ge$_{0.50}$ [5]	0.9977	4.75	0.2450	0.2380

Table 13 Interaxial ratio *c/a*, valence electron concentration VEC$_A$, contact distances between small atoms δ_{M-M}, and sum of the average covalent radii 2r_M for the solid solution PrAg$_{0.8}$Ge$_{1.2}$-PrAl$_{1.55-1.48}$Ge$_{0.45-0.52}$.

Composition	*c/a*	VEC$_A$	δ_{M-M}, nm	2r_M, nm
PrAg$_{0.80}$Ge$_{1.20}$ [2]	0.9340	4.30	0.2528	0.2536
PrAg$_{0.70}$Al$_{0.20}$Ge$_{1.10}$	0.9337	4.35	0.2524	0.2516
PrAg$_{0.50}$Al$_{0.50}$Ge$_{1.00}$	0.9593	4.50	0.2507	0.2480
PrAg$_{0.40}$Al$_{0.60}$Ge$_{1.00}$	0.9686	4.60	0.2495	0.2464
PrAg$_{0.38}$Al$_{0.80}$Ge$_{0.82}$	0.9611	4.53	0.2504	0.2454
PrAg$_{0.25}$Al$_{1.00}$Ge$_{0.75}$	0.9767	4.63	0.2497	0.2430
PrAg$_{0.10}$Al$_{1.30}$Ge$_{0.60}$	0.9792	4.70	0.2499	0.2400
PrAl$_{1.48}$Ge$_{0.52}$ [6]	0.9852	4.76	0.2495	0.2381

Table 14 Interaxial ratio *c/a*, valence electron concentration VEC$_A$, contact distances between small atoms δ_{M-M}, and sum of the average covalent radii $2r_M$ for the solid solution NdAg$_{0.7}$Ge$_{1.3}$-NdAl$_{1.63-1.50}$Ge$_{0.37-0.50}$.

Composition	*c/a*	VEC$_A$	δ_{M-M}, nm	$2r_M$, nm
NdAg$_{0.70}$Ge$_{1.30}$	0.9468	4.45	0.2496	0.2524
NdAg$_{0.60}$Al$_{0.20}$Ge$_{1.20}$	0.9572	4.50	0.2490	0.2504
NdAg$_{0.52}$Al$_{0.40}$Ge$_{1.08}$	0.9485	4.52	0.2504	0.2486
NdAg$_{0.42}$Al$_{0.60}$Ge$_{0.98}$	0.9610	4.57	0.2493	0.2466
NdAg$_{0.34}$Al$_{0.80}$Ge$_{0.86}$	0.9713	4.59	0.2485	0.2449
NdAg$_{0.20}$Al$_{1.10}$Ge$_{0.70}$	0.9725	4.65	0.2491	0.2420
NdAg$_{0.08}$Al$_{1.40}$Ge$_{0.52}$	0.9759	4.68	0.2491	0.2394
NdAl$_{1.50}$Ge$_{0.50}$ [7]	0.9795	4.75	0.2481	0.2380

Table 15 Interaxial ratio *c/a*, valence electron concentration VEC$_A$, contact distances between small atoms δ_{M-M}, and sum of the average covalent radii $2r_M$ for the compound SmAg$_{0.55-0.36}$Al$_{0.43-0.80}$Ge$_{1.02-0.84}$.

Composition	*c/a*	VEC$_A$	δ_{M-M}, nm	$2r_M$, nm
SmAg$_{0.55}$Al$_{0.43}$Ge$_{1.02}$	0.9543	4.46	0.2475	0.2489
SmAg$_{0.50}$Al$_{0.50}$Ge$_{1.00}$	0.9569	4.50	0.2471	0.2480
SmAg$_{0.48}$Al$_{0.60}$Ge$_{0.92}$	0.9552	4.48	0.2472	0.2474
SmAg$_{0.42}$Al$_{0.70}$Ge$_{0.88}$	0.9596	4.52	0.2468	0.2462
SmAg$_{0.36}$Al$_{0.80}$Ge$_{0.84}$	0.9662	4.56	0.2464	0.2451

Conclusions

AlB$_2$-type phases were observed in the systems {Ce,Pr,Nd,Sm}–Ag–Al–Ge at 873 K. In the systems with Ce, Pr, and Nd they form complete solid solutions between ternary compounds CeAg$_{0.8}$Ge$_{1.2}$–CeAl$_{1.6-1.5}$Ge$_{0.4-0.5}$, PrAg$_{0.8}$Ge$_{1.2}$–PrAl$_{1.55-1.48}$Ge$_{0.45-0.52}$, and NdAg$_{0.7}$Ge$_{1.3}$–NdAl$_{1.63-1.50}$Ge$_{0.37-0.50}$, whereas in the system with Sm a quaternary compound with a significant homogeneity range, SmAg$_{0.55-0.36}$Al$_{0.43-0.80}$Ge$_{1.02-0.84}$, is formed. The valence electron concentration per atom of the statistical mixture Ag+Al+Ge (VEC$_A$) is in the range 4.30-4.76. Increase of the Al and decrease of the Ag and Ge contents lead to shortening of the contact distances between small-size atoms in the infinite graphite-like planar nets perpendicular to the 6-fold axes.

Acknowledgements

References

[1] P.S. Salamakha, O.L. Sologub, O.I. Bodak, In: K.A. Gschneidner, Jr., L. Eyring (Eds.), *Handbook on the Physics and Chemistry of the Rare Earth*, Vol. 27, Elsevier, Amsterdam, 1999, pp. 1-224.

[2] I.A. Savysyuk, E.I. Gladyshevskii, R.E. Gladyshevskii, *J. Alloys Compd.* 314 (2001) 167-169.

[3] O.V. Zaplatynsky, P.S. Salamakha, O.L. Sologub, O.S. Procyk, O.I. Bodak, *Pol. J. Chem.* 70 (1996) 267-269.

[4] I. Melnyk, S. Pikus, V. Kuprysyuk, N. Semuso, R. Gladyshevskii, *Arch. Mater. Sci.* 26(4) (2005) 279-301.

[5] A.A. Muraveva, O.S. Zarechnyuk, *Izv. Akad. Nauk SSSR. Neorg. Mater.* (6) (1970) 1066-1068.

[6] E.I. Gladyshevskii, N.Z. Nakonechna, K. Cenzual, R.E. Gladyshevskii, J.-L. Jorda, *J. Alloys Compd.* 296 (2000) 265-271.

[7] A. Raman, H. Steinfink, *Inorg. Chem.* 6 (1967) 1789-1791.

[8] N. Muts, S. Pukas, O. Shcherban, L. Akselrud, R. Gladyshevskii, *Coll. Abstr. 15th Int. Conf. Solid Compd. Trans. Elements*, Kraków, 2006, p. 38.

[9] R.S. Kozak, V.M. Davydov, R.E. Gladyshevskii, *Coll. Abstr. 17th Ukr. Conf. Inorg. Chem.*, Lviv, 2008, p. 138.

[10] R.S. Kozak, R.E. Gladyshevskii, *Ukr. Khim. Zh.* 76(3) (2010) 3-9.

[11] R. Kozak, I. Labinska, R. Gladyshevskii, *Visn. Lviv. Univ., Ser. Khim.* (in press).

[12] R.A. Young, A.C. Larson, C.O. Paiva-Santos, *Rietveld analysis of X-ray and neutron powder diffraction patterns*, School of Physics, Georgia Institute of Technology, Atlanta, 1998.

[13] G.M. Sheldrick, *SHELX-97 – WinGX Version*, Release 97-2, University of Göttingen, Germany, 1997.

[14] E. Parthé, *Elements of Inorganic Structural Chemistry*, K. Sutter Parthé Publisher, Petit-Lancy, 1996, 170 p.